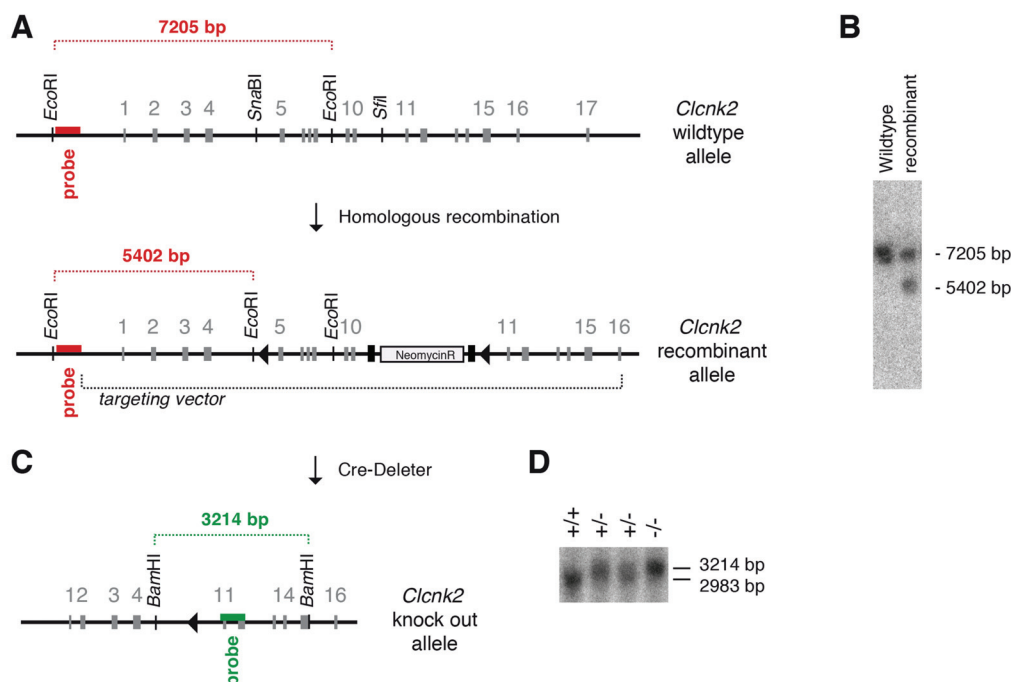


## Supplementary Material

### Supplementary figures



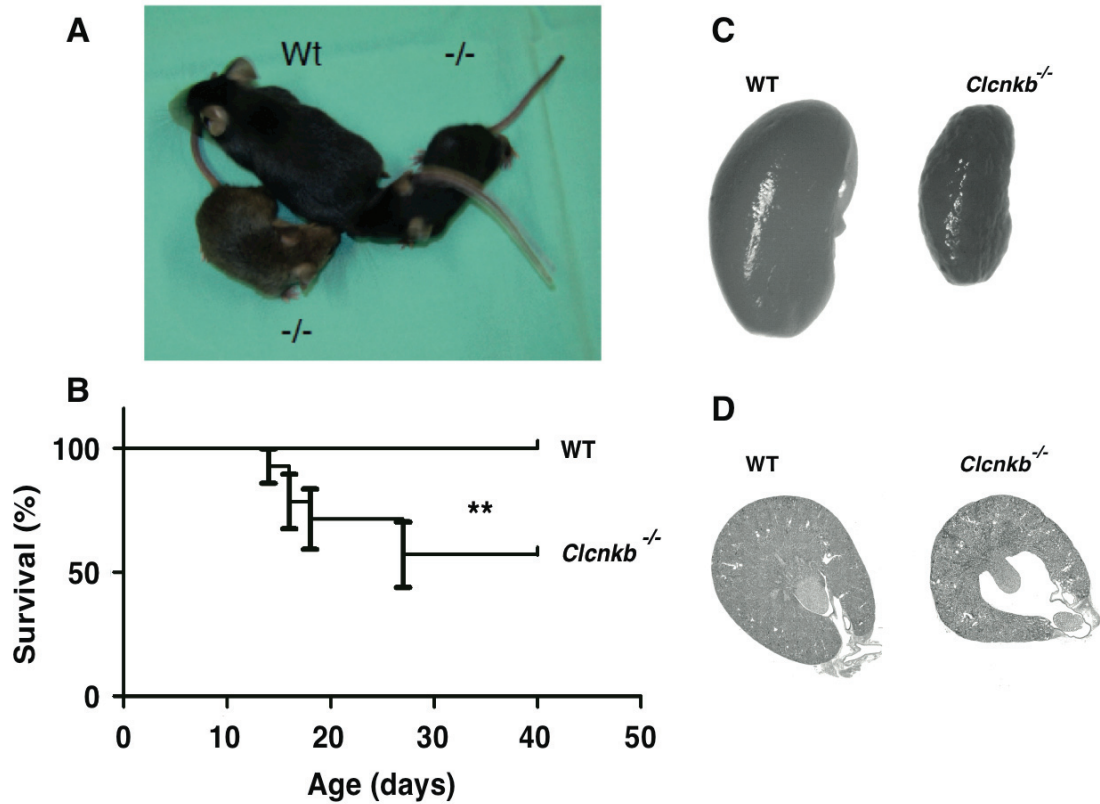
#### Supplementary figure 1: Inactivation of the murine *Clcnk2* gene

A - Partial genomic structure of the *Clcnk2* locus (top) and the targeted *Clcnk2* locus (below). The dotted line indicates the genomic sequence of the targeting vector. A neomycin resistance cassette flanked by *frt* sites (black boxes) and an additional loxP site (black triangle) were inserted into the *SfiI* site of intron 10. A second loxP site and an additional *EcoRI* site were inserted into the *SnaBI* site in intron 4. Binding sites of the external probe for Southern blot analysis highlighted in red.

B - Southern blot analysis of ES-cell clones with an external probe following restriction digest with *EcoRI*. The integration of the targeting vector by homologous recombination results in a shift of DNA fragment sizes from 7205 bp to 5402 bp

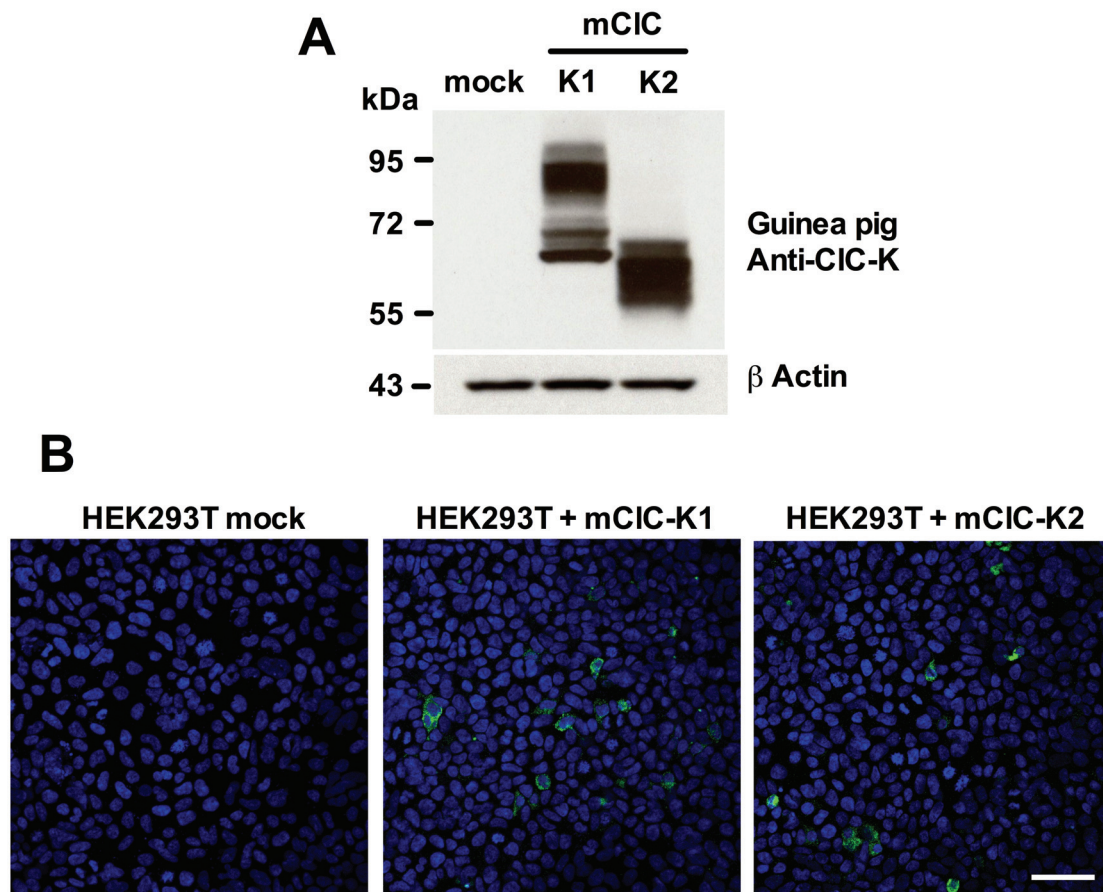
C - Generation of constitutive *Clcnk2*<sup>-/-</sup> mice by mating of floxed mice with Cre-Deleter mice. Cre recombinase activity results in the removal of exons 5 - 10 and the neomycin resistance cassette. Binding site of the internal probe for Southern blot analysis highlighted in green.

D - Southern blot genotyping of mice with an internal probe following restriction digest with *BamHI*. Removal of exons 5-10 results in a shift of DNA fragment sizes from 5572 bp to 3214 bp. Note that the shown *Clcnk2* wildtype fragment at 2983 bp originates from the C57BL/6 strain.



**Supplementary Figure 2: Disruption of the *Clcnk2* in mice results in early mortality and hydronephrosis**

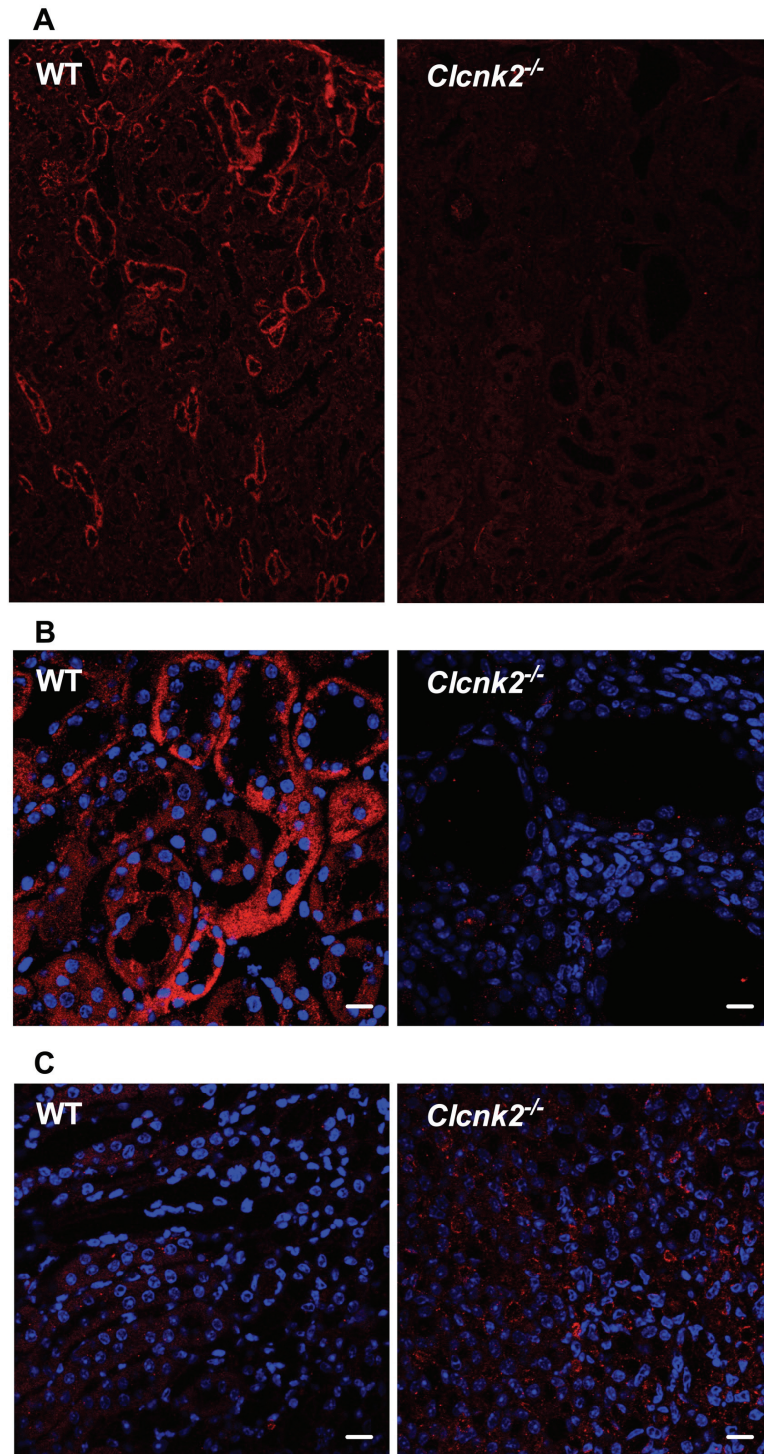
Mice inactivated for the *Clcnk2* gene have a reduced size and body weight (A). Survival rate is reduced with a half-life of about 5-6 weeks ( $n = 14/\text{group}$ )(B). Weight of kidney of *Clcnk2*<sup>-/-</sup> mice is reduced with a rough aspect (C). Hematoxylin and eosin stained whole kidney sections show massive hydronephrosis in *Clcnk2*<sup>-/-</sup> mouse.



**Supplementary figure 3: Characterization of a new antibody against CLC-K proteins**  
 A new antibody raised in guinea pig against CLC-K proteins as described in *detailed methods*

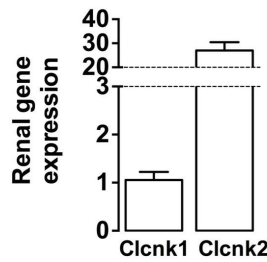
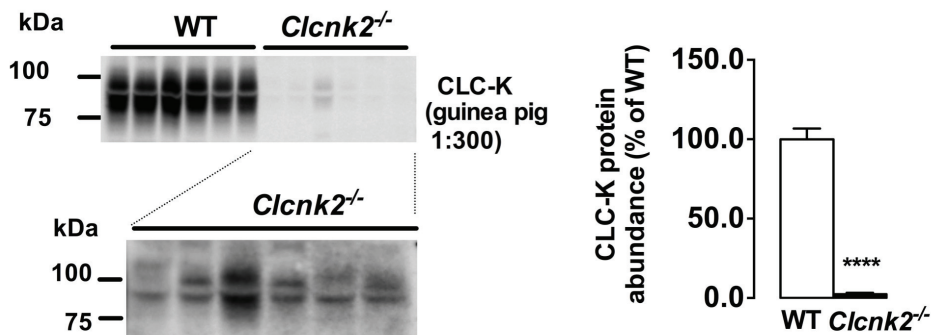
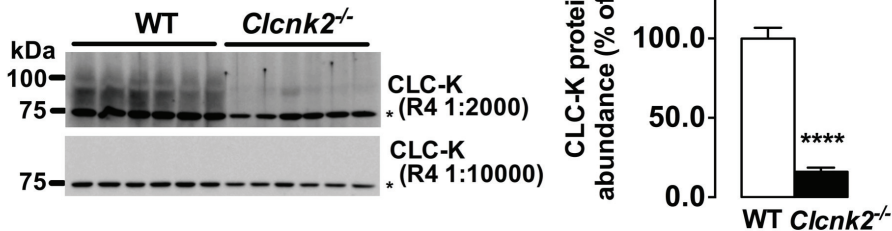
A – Western blotting using the guinea pig anti-CLC-K antibody in HEK293T cells transfected with a vector overexpressing mouse Barttin / mouse CLC-K1 (K1) or mouse Barttin / mouse CLC-K2 (K2) and untransfected HEK293T cells (mock).

B – Immunofluorescence in HEK293T cells transfected with a vector overexpressing mouse Barttin / mouse CLC-K1 (middle panel) or mouse Barttin / mouse CLC-K2 (right panel) and untransfected HEK293T cells (left panel). Scale bar: 60  $\mu$ m. Both CLC-K channels are recognized by the new guinea pig anti-CLC-K antibody, which does not detect any signal on untransfected HEK293T cells.



**Supplementary Figure 4: Localization of CLC-K with Rabbit anti CLC-K R4 antibody<sup>1,2</sup>.**

A - Low magnification of the renal cortex of *Clcnk2*<sup>+/+</sup> and *Clcnk2*<sup>-/-</sup> mice stain with the "R4" antibody. B - In the cortex, R4 antibody stains the basolateral membrane of thick ascending limbs (TAL), distal convoluted tubules (DCT), and intercalated cells of the collecting duct (bar = 25 $\mu$ m). "R4" signal is absent from the renal cortex of *Clcnk2*<sup>-/-</sup> mice. C - In the renal medulla (at the border between the outer and inner medulla) from *Clcnk2*<sup>-/-</sup> mouse a very weak staining is detected in mTALs. Scale bars = 25  $\mu$ M.

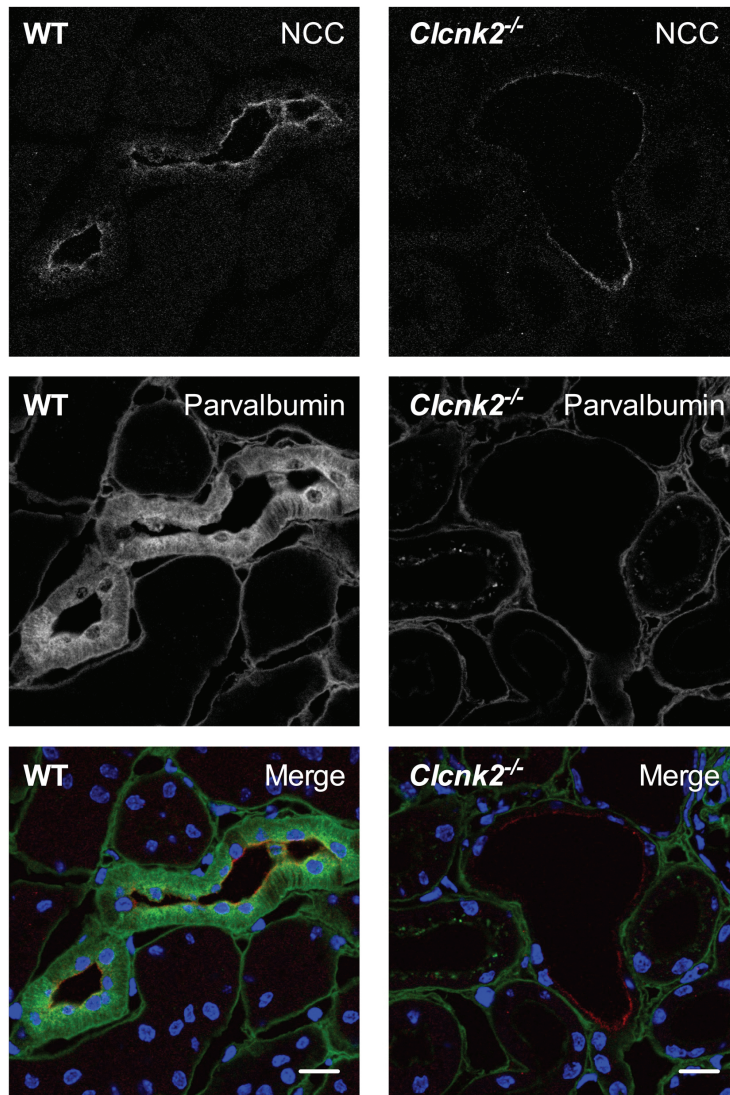
**A****B****C**

**Supplementary Figure 5: Renal expression and abundance of CLC-K in *Clcnk2*<sup>+/+</sup> and *Clcnk2*<sup>-/-</sup> mice**

A – Quantitative PCR was used to assess *Clcnk1* and *Clcnk2* gene expression in adult WT mouse kidneys (n=5)

B – The newly generated guinea pig antibodies against CLC-K proteins recognized polypeptides migrating between ~70 and 100 kDa when used for immunoblotting on kidney lysates from WT. 70 and 100 kDa signals in *Clcnk2*<sup>-/-</sup> mouse lysates was barely absent and were quantified by densitometric analysis (n=6; \*\*\*\* p<0.0001). Longer exposition (lower panel of B) of *Clcnk2*<sup>-/-</sup> mouse lysates revealed a similar pattern of expression than in WT.

C R4 antibody generated in rabbit<sup>1, 2</sup> against CLC-K proteins also recognized polypeptides migrating between ~70 and 100 kDa when used for immunoblotting on kidney lysates from WT. 70 and 100 kDa signals in *Clcnk2*<sup>-/-</sup> mouse lysates was barely absent and were quantified by densitometric analysis (n=6; \*\*\*\* p<0.0001). Two different dilutions for the R4 antibody were used. 1:2000 dilution was necessary to detected CLC-K protein



**Supplementary Figure 6: Colocalization of NCC and parvalbumin in *Clcnk2*<sup>-/-</sup> mice**  
 NCC (upper panel) and Parvalbumin (middle panel) localization in kidney sections from WT and *Clcnk2*<sup>-/-</sup> mice. Merging of the separate channels is shown in bottom panel (green : Parvalbumin and red : NCC). Parvalbumin expression was barely detectable in *Clcnk2*<sup>-/-</sup> mouse kidneys. As shown also in Figure 3, most DCT from *Clcnk2*<sup>-/-</sup> mice were abnormal with flatten epithelium and dilated tubules. Basal membranes are also stained during parvalbumin labeling. Indee, primary antibody against parvalbumin was a mouse monoclonal antibody. Secondary antibody against mouse IgG recognized this primary antibody and also recognized endogenous kidney immunoglobulins from the basal membranes.

## **Supplementary tables**

Anion	ClC-K2 candidate			Pseudo CFTR		
	G (pS)	V <sub>reversal</sub> (mV)	P <sub>X</sub> /P <sub>Cl</sub>	G (pS)	V <sub>reversal</sub> (mV)	P <sub>X</sub> /P <sub>Cl</sub>
Cl <sup>-</sup>	12.2 ± 1.3 (6)	1.0 ± 0.77 (6)	-			
Br <sup>-</sup>	6.0 ± 1.0 (9)	-13.3 ± 1.8 (9)	0.58 ± 0.06 (9)			
NO <sub>3</sub> <sup>-</sup>	7.7 ± 1.0 (7)	-11.8 ± 1.7 (7)	0.62 ± 0.05 (7)	7.6 (2)	12.9 (2)	1.89 (2)
I <sup>-</sup>	6.5 ± 2.2 (4)	1.5 ± 1.0 (4)	1.1 ± 0.05 (4)	8.2 (1)	13.4 (1)	1.93 (1)

### **Supplementary table 1: Anion selectivity of Cl<sup>-</sup> channels in the TAL.**

The precise typology of chloride channels in the TAL remains ambiguous. On the one hand, we described a 10-pS Cl<sup>-</sup> channel with NO<sub>3</sub><sup>-</sup> > Br<sup>-</sup> > Cl<sup>-</sup> anion selectivity sequence, which is incompatible with ClC-K anion selectivity<sup>3-5</sup>. This channel was coined as pseudo-CFTR because of its functional similarities to CFTR<sup>5</sup>. On the other hand, immunofluorescence studies<sup>6</sup> strongly support the presence of ClC-K2 in the TAL, suggesting that we failed to record ClC-K2-like channels in these previous experiments because of distinct experimental conditions<sup>7</sup>. This was clarified in a series of experiments performed on C57/BL6 mice. We patched the basolateral membranes of CTAL fragments using NaCl in the pipette, and excised the patches for testing the effects of Cl<sup>-</sup>, Br<sup>-</sup> and NO<sub>3</sub><sup>-</sup> in conditions favoring the activity of ClC-K2 candidate channels (see detailed Methods). As expected, the results showed the presence of two channels with distinct anion selectivity, one being compatible with ClC-K2-like channels<sup>8,9</sup> and the other with pseudo-CFTR (Supplementary Table 1). This second channel is far less frequent than ClC-K2 candidate in the present experimental conditions (3 of 14 patches with Cl<sup>-</sup> channel activity).

<b>Part of the renal tubule</b>	<b>status</b>	<b><i>f</i></b>	<b><i>G</i> (pS)</b>
DCT [2]	WT (9)	0	NA
DCT [3]	KO (13)	0	NA
CNT/CCD [4]	WT (24)	0.20	37.7 ± 4.0 (5)
CNT/CCD [3]	KO (10)	0.10	33.7 (1)
CTAL [3]	WT (14)	0.14	41.2 (2)
CTAL [2]	KO (13)	0.08	35.6 (1)

**Supplementary table 2: Distribution of ClC-K1 in the DCT and TAL of *Clcnk2*<sup>+/+</sup> and *Clcnk2*<sup>-/-</sup> mice.** [n] indicates the number of mice used in the experiments; (n), the number of measurements; *f*, the frequency of finding an active channel; *G*, the unit conductance.



		<i>Clcnk2<sup>+/+</sup></i>	<i>Clcnk2<sup>-/-</sup></i>
<b>Blood</b>	[Na <sup>+</sup> ], mM	148 ± 1 (7)	138 ± 2 (8)***
	[K <sup>+</sup> ], mM	4.73 ± 0.12 (7)	3.37 ± 0.17 (8)****
	[Cl <sup>-</sup> ], mM	111 ± 1 (7)	79 ± 5 (8)****
	Hematocrit, %	42.5 ± 0.8 (6)	49 ± 1.4 (8)**
	pH	7.34 ± 0.02 (7)	7.53 ± 0.02 (8)****
	[HCO <sub>3</sub> <sup>-</sup> ], mM	22.4 ± 0.7 (7)	45.3 ± 3.6 (8)****
	pCO <sub>2</sub> , mmHg	44.8 ± 1.8 (7)	58.1 ± 2.9 (8)**
	Food intake, g/24h	3.6 ± 0.3 (14)	2.7 ± 0.2 (5)
Body weight, g	22.6 ± 0.7 (14)	10.4 ± 0.8 (5)****	
<b>Urine</b>	Osmolality, mOsm/L	3371 ± 339 (14)	769 ± 39 (5)****
	Urine volume, mL/24h	4.6 ± 0.2 (14)	7.0 ± 0.6 (5)****
	Na <sup>+</sup> /Creatinine, mM/mM	25.8 ± 1.8 (14)	22.0 ± 2.9 (5)
	K <sup>+</sup> /Creatinine, mM/mM	81.8 ± 6.0 (14)	69.3 ± 4.2 (5)
	Ca <sup>++</sup> /Creatinine, mM/mM	0.63 ± 0.10 (14)	0.64 ± 0.11 (5)
	Mg <sup>++</sup> /Creatinine, mM/mM	8.24 ± 0.66 (14)	11.60 ± 0.55 (5) **
	PGE <sub>2</sub> /Creatinine, nM/mM	0.89 ± 0.11 (7)	6.64 ± 1.33 (5)****
	Aldosterone/Creatinine nM/mM	3.73 ± 0.33 (6)	3.18 ± 1.20 (5)

### Supplementary Table 3 : Physiological datas from *Clcnk2<sup>-/-</sup>* and WT

Blood was collected by retro-orbital puncture. Electrolytes and other parameters were immediately measured. Urine was collected for 24hours in metabolic cages and parameters were measured as explained in detailed methods.

Data are means ± S.E. Mice number for each parameter is indicated in brackets. Statistical significance was only assessed vs. WT fed same diet, using a two-tailed unpaired Student's *t*-test. \*\*\*\* p<0.0001 ; \*\*\* : p<0.001 ; \*\* : p<0.01

## **Detailed methods**

### ***Generation of *Clcnk2* deficient mice.***

A BAC clone (bMQ222b04, Source Bioscience, Nottingham, United Kingdom) was used to construct the targeting vector. An approximately 13kb fragment including exons 1-16 of the *Clcnk2* gene was cloned by recombineering into the pKO-V901 plasmid (Lexicon Genetics, The Woodlands, TX, USA) with a phosphoglycerate kinase (pgk) promoter-driven diphtheria toxin A cassette. A pgk promoter-driven neomycin resistance cassette flanked by *frt* sites and an additional *loxP* site was inserted into the *SfiI* site of intron 10. A second *loxP* site and an additional *EcoRI* site were inserted into the *SnaBI* site in intron 4. The construct was linearized with *NotI* and electroporated into R1 mouse embryonic stem (ES) cells. Neomycin-resistant clones were analyzed by Southern blot using *EcoRI* and an external 646-bp probe (UCSC Genome Browser GRCm38/mm10, *Mus musculus* chromosome 4, 141417454-141418099). Two correctly targeted ES cell clones were injected into C57BL/6 blastocysts to generate chimeras. Chimeric mice were mated to a cre-Deleter mouse strain to remove exons 5-10 and the selection cassette<sup>10</sup>. Studies were performed in a mixed 129Sv/C57BL/6 background in the F5 and F6 generation. Genotypes were determined by PCR of tail biopsy DNA. For PCR genotyping, the forward primer F1 (5'-gtgagacctggagacctgat-3') and the reverse primers R1 (5'-cccactttcgatcttccgtaaag-3') and R2 (5'-ggagtttctgtgccttgtga-3') were used in a single PCR mix. In C57BL/6 mice the primer pair F1/R1 amplified a 523-bp wildtype allele, and the primer pair F1/R2 a 586-bp KO allele.

### ***Isolation of renal tubules for patch analysis, solutions and chemicals***

Tubular fragments were isolated from the kidneys after collagenase treatment (Worthington CLS II, 300 U/ml) as described previously<sup>8,11</sup>.

The tubules were bathed in physiological saline solution containing (in mM) 140 NaCl, 4.8 KCl, 1 CaCl<sub>2</sub>, 1.2 MgCl<sub>2</sub>, 10 glucose, 10 HEPES and adjusted to pH 7.4 with NaOH. The patch pipettes were filled with a high-K<sup>+</sup> solution containing (in mM) 144.8 KCl, 1 CaCl<sub>2</sub>, 1 MgCl<sub>2</sub>, 10 HEPES, adjusted to pH 7.4 with KOH when we wished to record simultaneously K<sup>+</sup> and Cl<sup>-</sup> channels. The patch pipettes were filled with a solution containing (in mM): 145 NMDGCl, 1 CaCl<sub>2</sub>, 1.2 MgCl<sub>2</sub>, 10 glucose, 10 HEPES and adjusted to pH 7.4 with NMDG when we wished to record only Cl<sup>-</sup> channels. For measuring the relative anion permeabilities, the pipette was filled with a solution containing (in mM): 140 NaCl, 5 KCl, 1 CaCl<sub>2</sub>, 1.2 MgCl<sub>2</sub>, 10 glucose, 10 HEPES and adjusted to pH 7.4 with NaOH. For determining anion selectivity, the excised patches were initially superfused with a physiological saline solution (see above) devoid of any CaCl<sub>2</sub> and supplemented with 2 mM EGTA and 1 mM ATP. Test solutions were similar except that 130 mM NaCl was replaced by NaBr, NaNO<sub>3</sub> or NaI.

### ***Current recordings***

Single-channel currents were recorded from patches of basolateral membranes using the cell-attached and excised, inside-out configurations of the patch-clamp technique. Patch-clamp pipettes were coated with Sylgard and polished just before use. Currents were recorded with List LM-EPC7 or Bio-logic RK 400 patch-clamp

amplifiers, and monitored and analyzed using Pclamp 10 software (Molecular Devices, California, USA). In the cell-attached configuration, the clamp potential applied with respect to the bath ( $V_c$ ) is superimposed on the spontaneous membrane potential. The experiments were carried out at room temperature (22-27 °C).

In the DCT, the patch-clamp recordings were done at the beginning of the DCT, after the post-macula densa short TAL-like segment, in order to patch DCT1 cells. We used  $K^+$ -rich pipette solutions, which allows recording simultaneously (on the same patch)  $K^+$  and  $Cl^-$  channels, and ensures that the absence of  $Cl^-$  channels is not due to vesicle seal-types.  $K^+$  channel activity was recorded over a large range of negative and positive potentials (mostly between -100 and +60 mV) and  $Cl^-$  channels mainly at positive potentials between +50 and +120 mV where the  $K^+$  currents have a low amplitude or are absent (around the inversion potential for  $K^+$  channels, i.e. +80 mV). This protocol is useable because the DCT1 is endowed with only one type of  $Cl^-$  channel<sup>8</sup> (ClC-K2 candidate) and one type of  $K^+$  channel<sup>12</sup> (Kir4.1/Kir5.1). In the intercalated cells of CNT/CCD and in the TAL, we used NMDGCl solution in the pipette solution for eliminating  $K^+$  currents.

### **Patch data analysis**

Single-channel current recordings were filtered at 700 Hz low-pass ( $K^+$  channels) or 300Hz ( $Cl^-$  channel) by an 8-pole Bessel filter (LPBF-48DG, NPI Electronic, Tamm, Germany) and digitized at a sampling rate of 3 kHz using a Digidata 1200 analog-to-digital converter and Axoscope software (Axon Instruments). Chloride channel activity ( $NP_o$ ) was measured from digitized stretches of recording lasting at least 30 seconds using Clampfit software as follows: the time-averaged current passing through the channels on the patch,  $\langle I \rangle$ , was calculated from mean current taking the closed current level as reference and divided by the amplitude of the unit current ( $i$ ), thus yielding the  $NP_o$  according to the equation  $\langle I \rangle = NP_o \cdot i$ . The closed current level was determined taking advantage of the high sensitivity to protons of the channel. At the end of the recording, we superfused the tubular fragment with a bath solution containing 20 mM sodium acetate<sup>8</sup>. This manoeuvre induces intracellular acidification. The apparent number of simultaneously open channels was determined by a visual inspection of the whole recording and secondarily allowed to calculate an apparent  $P_o$ .

The closed current level for  $K^+$  channel could be determined by visual inspection because of the low  $P_o$ . For  $K^+$  channel, the unit conductance was measured as a slope conductance for inward currents ( $g_{in}$ ). For  $Cl^-$  channel, the unit conductance was measured as a slope conductance for currents over the whole range of tested potentials. The relative permeabilities to anions were calculated from the reversal potential in each condition using the voltage Goldman-Hodgkin-Katz equation<sup>12</sup>.

### **Renal function**

All animal experiments were approved by the Thüringer Landesamt für Lebensmittelsicherheit und Verbraucherschutz (TLLV) in Germany.

5-8 week-old *Clcnk2*<sup>+/+</sup> (WT), and *Clcnk2*<sup>-/-</sup> littermates mice were explored for their renal function. For urine collection, mice were housed individually in metabolic cages (Tecniplast, France). 24-hour urine was collected after careful habituation. Urinary

creatinine concentrations were measured with the Jaffe method on microtiter plates. Blood was collected by retroorbital puncture. Blood pH and pCO<sub>2</sub> were measured with the ABL77 pH/blood-gas analyzer (Radiometer, Copenhagen, Denmark) as well as blood sodium, blood potassium, blood chloride and hematocrit. Blood bicarbonate concentration was calculated from pH and pCO<sub>2</sub> using the Henderson-Hasselbalch equation. Urinary calcium and magnesium were measured by atomic absorption spectrophotometry (Perkin Elmer Apparatus, Model 3110, Cortabeuf, France). Urinary sodium and potassium were measured by flame photometry (IL943, Instruments Laboratory, Lexington, MA). 24-hour urinary aldosterone excretion was measured via RIA (DPC Dade Behring). 24-hour PGE<sub>2</sub> excretion was measured with a Prostaglandin E<sub>2</sub> ELISA Kit (Cayman chemical, reference 514010). Urine osmolality was determined with a freezing point osmometer (Roebbling, Berlin, Germany)

### ***Hydrochlorothiazide or furosemide sensitivity tests***

Hydrochlorothiazide (HCTZ, Sigma-Aldrich, 50mg/kg body weight) or furosemide (Sigma-Aldrich, 2mg/kg body weight) were injected in the peritoneum of *Clcnk2*<sup>+/+</sup> and *Clcnk2*<sup>-/-</sup> mice housed in metabolic cages. 3-hour urine output was collected after injection and further analyzed for sodium and creatinine content as described above. The day prior to the HCTZ or furosemide test, a 3-hour control period was performed after vehicle injection to assess basal 3-hour natriuresis.

### ***Cell culture***

HEK293T cells were grown in DMEM (Gibco, Invitrogen) supplemented with 10 % fetal bovine serum, Penicillin (100 IU/ml) and Streptomycin (100 mg/ml) at 37 °C in 5 % CO<sub>2</sub>. HEK293T cells were untransfected or transiently transfected using XtremGene9 DNA transfection reagent, according to Manufacturer's instructions, with a bicistronic vector containing the coding sequences of mouse Barttin and mouse CIC-K1 or CIC-K2. Forty hours after transfection, cells were either fixed by incubation with 4% paraformaldehyde solution and subjected to immunofluorescence assay, or lysed in a 1 % Triton-X100 lysis buffer supplemented with a protease inhibitor mix (CComplete, Roche Diagnostic) for total protein extraction followed by immunoblotting.

### ***Immunoblots***

Total kidneys were homogenized in ice-cold isolation buffer (250 mM sucrose, 20 mM Tris–Hepes, pH 7.4) enriched with protease inhibitor cocktail (complete, Roche Diagnostics, Risch, Switzerland), and anti-phosphatase inhibitor cocktail (Roche) and pepstatin A (1.5 µg/ml). Protein lysate preparation and immunoblotting procedures were performed as described previously<sup>13</sup>. Quantification of each band was performed via densitometry using ImageJ.

### ***Immunofluorescence studies***

All immunostainings were performed on renal sections of at least 3 independent mice per genotype if not indicated otherwise and only representative findings are presented in the figures. Kidneys were fixed by *in vivo* perfusion of 4% paraformaldehyde in phosphate buffer. Kidney blocks were frozen in isopentane

cooled by liquid nitrogen. 4  $\mu$  m cryosections were stained with primary and secondary antibodies as listed below and analyzed with a laser scanning microscope (Zeiss LSM 710).

### ***Antibodies***

Primary antibodies: guinea pig anti mouse Ae1<sup>14</sup> (Immunofluorescence 1:5000), guinea pig anti mouse pendrin<sup>15</sup> (Immunofluorescence 1:10000), rabbit anti NKCC2<sup>16</sup> (Immunofluorescence 1:20000 ; Immunoblot 1:10000), rabbit anti NCC<sup>17</sup> (Immunofluorescence 1:2000 ; Immunoblot 1:10000), rabbit anti phosphorylated Tyr53 NCC<sup>17</sup> (Immunofluorescence 1:20000 ; Immunoblot &:10000), rabbit anti phosphorylated NKCC2<sup>18</sup> (Immunofluorescence 1:10000 ; Immunoblot 1:5000), rabbit anti Renin<sup>19</sup> (1:20000), rabbit anti CLC-K (R4 ; Immunofluorescence 1:2000 , Immunoblot 1:2000 & 1:10000). A new antibody against CLC-K proteins was raised in guinea pig with the following peptide (MEELVGLREGSSKCP-C, coupled to BSA). Antibodies were affinity-purified against the peptide used for immunization. Dilution for immunofluorescence was 1:2000 and 1:1000 for immunoblotting. Secondary antibodies for immunofluorescence were goat anti rabbit coupled with Alexa 555 (Invitrogen, Karlsruhe, Germany 1:2000) and donkey anti guinea pig cy5 (Jackson laboratories, 1:800). DAPI (Invitrogen, Karlsruhe, Germany) was used to localize the nuclei.

### ***Renin gene expression***

Frozen kidneys were homogenized with mortar and pestle and RNA was isolated using TRIzol reagent (Invitrogen Life Technologies, Carlsbad, CA, USA) following the instructions of the manufacturer. 5  $\mu$ g total RNA (whole kidney) were reverse transcribed with SuperScript III Reverse Transcriptase (Invitrogen Life Technologies, Carlsbad, CA, USA). Duplicate qPCR reactions were performed with SsoFast EvaGreen Supermix (BioRad, Hercules, CA, USA) using a CFX96 Touch Real-Time PCR Cycler (BioRad, Hercules, CA, USA). Primer sequences were Ren1\_for (5'-atctttgacacgggttcagc-3'), Ren1\_rev (5'-tgatccgtagtgatggtga-3') and the ActB Quantitect Primer Assay QT01136772 (Qiagen, Hilden, Germany).

### ***Statistics***

Unless otherwise indicated statistical significance was tested with Student's t-test and values are mean  $\pm$  SEM.

## **Supplementary Material References**

1. Kieferle, S, Fong, P, Bens, M, Vandewalle, A, Jentsch, TJ: Two highly homologous members of the ClC chloride channel family in both rat and human kidney. *Proc Natl Acad Sci U S A*, 91: 6943-6947, 1994.
2. Vandewalle, A, Cluzeaud, F, Bens, M, Kieferle, S, Steinmeyer, K, Jentsch, TJ: Localization and induction by dehydration of ClC-K chloride channels in the rat kidney. *Am J Physiol*, 272: F678-688, 1997.
3. Guinamard, R, Chraïbi, A, Teulon, J: A small-conductance Cl<sup>-</sup> channel in the mouse thick ascending limb that is activated by ATP and protein kinase A. *J Physiol*, 485 ( Pt 1): 97-112, 1995.
4. Guinamard, R, Paulais, M, Teulon, J: Inhibition of a small-conductance cAMP-dependent Cl<sup>-</sup> channel in the mouse thick ascending limb at low internal pH. *J Physiol*, 490 ( Pt 3): 759-765, 1996.
5. Marvao, P, De Jesus Ferreira, MC, Bailly, C, Paulais, M, Bens, M, Guinamard, R, Moreau, R, Vandewalle, A, Teulon, J: Cl<sup>-</sup> absorption across the thick ascending limb is not altered in cystic fibrosis mice. A role for a pseudo-CFTR Cl<sup>-</sup> channel. *J Clin Invest*, 102: 1986-1993, 1998.
6. Kobayashi, K, Uchida, S, Mizutani, S, Sasaki, S, Marumo, F: Intrarenal and cellular localization of CLC-K2 protein in the mouse kidney. *J Am Soc Nephrol*, 12: 1327-1334, 2001.
7. Teulon, J, Lourdel, S, Nissant, A, Paulais, M, Guinamard, R, Marvao, P, Imbert-Teboul, M: Exploration of the basolateral chloride channels in the renal tubule using. *Nephron Physiol*, 99: p64-68, 2005.
8. Lourdel, S, Paulais, M, Marvao, P, Nissant, A, Teulon, J: A chloride channel at the basolateral membrane of the distal-convoluted tubule: a candidate ClC-K channel. *J Gen Physiol*, 121: 287-300, 2003.
9. Nissant, A, Paulais, M, Lachheb, S, Lourdel, S, Teulon, J: Similar chloride channels in the connecting tubule and cortical collecting duct of the mouse kidney. *Am J Physiol Renal Physiol*, 290: F1421-1429, 2006.
10. Schwenk, F, Baron, U, Rajewsky, K: A cre-transgenic mouse strain for the ubiquitous deletion of loxP-flanked gene segments including deletion in germ cells. *Nucleic Acids Res*, 23: 5080-5081, 1995.
11. Teulon, J, Paulais, M, Bouthier, M: A Ca<sup>2+</sup>-activated cation-selective channel in the basolateral membrane of the cortical thick ascending limb of Henle's loop of the mouse. *Biochim Biophys Acta*, 905: 125-132, 1987.
12. Lourdel, S, Paulais, M, Cluzeaud, F, Bens, M, Tanemoto, M, Kurachi, Y, Vandewalle, A, Teulon, J: An inward rectifier K(+) channel at the basolateral membrane of the mouse distal convoluted tubule: similarities with Kir4-Kir5.1 heteromeric channels. *J Physiol*, 538: 391-404, 2002.
13. Eladari, D, Cheval, L, Quentin, F, Bertrand, O, Mouro, I, Cherif-Zahar, B, Cartron, JP, Paillard, M, Doucet, A, Chambrey, R: Expression of RhCG, a new putative NH<sub>3</sub>/NH<sub>4</sub>(+) transporter, along the rat nephron. *J Am Soc Nephrol*, 13: 1999-2008, 2002.
14. Stehberger, PA, Shmukler, BE, Stuart-Tilley, AK, Peters, LL, Alper, SL, Wagner, CA: Distal renal tubular acidosis in mice lacking the AE1 (band3) Cl<sup>-</sup>/HCO<sub>3</sub><sup>-</sup> exchanger (slc4a1). *J Am Soc Nephrol*, 18: 1408-1418, 2007.

15. Hafner, P, Grimaldi, R, Capuano, P, Capasso, G, Wagner, CA: Pendrin in the mouse kidney is primarily regulated by Cl<sup>-</sup> excretion but also by systemic metabolic acidosis. *Am J Physiol Cell Physiol*, 295: C1658-1667, 2008.
16. Wagner, CA, Loffing-Cueni, D, Yan, Q, Schulz, N, Fakitsas, P, Carrel, M, Wang, T, Verrey, F, Geibel, JP, Giebisch, G, Hebert, SC, Loffing, J: Mouse model of type II Bartter's syndrome. II. Altered expression of renal sodium- and water-transporting proteins. *Am J Physiol Renal Physiol*, 294: F1373-1380, 2008.
17. Picard, N, Trompf, K, Yang, CL, Miller, RL, Carrel, M, Loffing-Cueni, D, Fenton, RA, Ellison, DH, Loffing, J: Protein phosphatase 1 inhibitor-1 deficiency reduces phosphorylation of renal NaCl cotransporter and causes arterial hypotension. *J Am Soc Nephrol*, 25: 511-522, 2014.
18. Gimenez, I, Forbush, B: Short-term stimulation of the renal Na-K-Cl cotransporter (NKCC2) by vasopressin involves phosphorylation and membrane translocation of the protein. *J Biol Chem*, 278: 26946-26951, 2003.
19. Menard, J, N'Goc, PW, Bariety, J, Guyenne, PT, Corvol, P: Direct radioimmunoassay and immunocytochemical localization of renin in human kidneys. *Clin Sci (Lond)*, 57 Suppl 5: 105s-108s, 1979.